Intra- and interannual variability of nearshore phytoplankton biovolume and community changes in the northern Humboldt Current system

NOEMI OCHOA[1], MARC H. TAYLOR[2]*, SARA PURCA[3] AND ELMER RAMOS[1]

[1]FACULTAD DE CIENCIAS BIOLOGICAS, UNIVERSIDAD NACIONAL MAYOR DE SAN MARCOS (UNMSM), AV. VENEZUELA, CDRA. 34, LIMA 100, PERU, [2]ALFRED WEGENER INSTITUTE FOR POLAR AND MARINE RESEARCH, AM HANDELSHAFEN 12, 27570 BREMERHAVEN, GERMANY AND [3]INSTITUTO DEL MAR DEL PERU (IMARPE), ESQ. GAMARRA Y VALLE S/N, APARTADO 22, CALLAO, PERU

*CORRESPONDING AUTHOR: marchtaylor@yahoo.com

Received November 15, 2009; accepted in principle February 7, 2010; accepted for publication February 9, 2010

Corresponding editor: William K.W. Li

Phytoplankton biomass in the northern Humboldt Current system is known to fluctuate over intra- and interannual time scales in response to environmental variability. General changes in the phytoplankton community are known, but a quantitative description of the link between environmental signals and observed changes is lacking. The present study examines these links through an analysis of long-term phytoplankton community changes in Ancon Bay, Peru (~11°S) from 1992 to 2004. The correlation of several environmental signals with phytoplankton biovolume was explored using stepwise multiple regression and community analyses. Results indicate that environmental signals of interannual periodicity, e.g. those most associated with the El Niño Southern Oscillation, were responsible for overall biovolume levels, while signals of annual periodicity (i.e. sea surface temperature) correlated to changes in phytoplankton taxa proportions. Specifically, diatoms (e.g. *Chaetoceros* spp., *Actinocyclus octonarius* and *Skeletonema costatum*) dominate biovolume only during the coldest periods (13–16°C) when upwelling is strongest, whereas dinoflagellates dominate warmer periods. During warm periods, a decrease in offshore transport or the intrusion of offshore waters (e.g. from beyond the shelf) increases the proportion of later phytoplankton successional stages, within the bay (e.g. dinoflagellates, flagellates and silicoflagellates). These results suggest that cross-shelf interactions between offshore and nearshore habitats exist at both intra- and interannual scales as affected by local upwelling variability, with possible consequences for resources of the nearshore upwelling ecosystem.

KEYWORDS: phytoplankton; coastal upwelling; El Niño phenomena; environmental effects; Eastern boundary currents; Ancon Bay; Peru; Humboldt Current

INTRODUCTION

The northern Humboldt Current system (NHCS) is recognized as one of the most productive ecosystems in the world (Fréon *et al.*, 2009). The NHCS's location near the equator allows for strong upwelling under relatively moderate wind forcing, which helps to maintain a

doi:10.1093/plankt/fbq022, available online at www.plankt.oxfordjournals.org. Advance Access publication March 12, 2010

stable, shallow thermocline where the plankton community can develop (Bakun, 1996; Bakun and Weeks, 2008). These physical attributes have helped to explain the "Peruvian puzzle" to fish production, whereby it produces 3–10× more fish than other upwelling ecosystems (Cury *et al.*, 1998; Fréon *et al.*, 2009).

Upwelling in eastern boundary current systems is driven by along-shore winds that push coastal waters offshore and allow deeper, nutrient-rich water to be upwelled to the surface where it can be used by primary producers. Seasonal wind variability exists in the NHCS, and remote changes in the trade winds also have been suggested to influence intra-annual changes in upwelling rate and thermocline depth (Myers, 1979; Goldberg and O'Brien, 1981; Chavez *et al.*, 1989); yet, this variability is generally thought to be of lower magnitude than in the southern Humboldt Current system (Montecinos *et al.*, 2003; Montecino and Lange, 2009). However, the low latitude location of the NHCS in the eastern Pacific makes it susceptible to high interannual environmental variability from the El Niño Southern Oscillation (ENSO).

Under neutral ENSO conditions, equatorial trade winds blow across the tropical Pacific and build up warm surface water in the west. This accumulation of surface water effectively pushes down the thermocline while the thermocline in the eastern Pacific is much shallower. Interannual ENSO variability is caused by changes in these large scale trade winds, whereby a relaxation or strengthening can result in a warm "El Niño" or a cold "La Niña" phase, respectively (Philander, 1990). During El Niño events, the relaxation of trade winds produces a Kelvin wave that travels eastward across the Pacific and is reflected along the coast of the Americas. In the NHCS, the normally shallow thermocline is pressed downward and upwelling no longer draws the cool, nutrient-rich waters to the photic zone, which results in decreased phytoplankton biomass and productivity. Strong, sustained El Niño events have been shown to reduce the size of the entire ecosystem up to the highest trophic levels through bottom-up limitations of available energy (Tam *et al.*, 2008; Taylor *et al.*, 2008).

Fluctuations in phytoplankton biomass have been linked to both intra- and interannual environmental variability through direct observations of *in situ* samples (Montecino *et al.*, 2006; Pennington *et al.*, 2006; Echevin *et al.*, 2008), remote sensing estimates (Thomas *et al.*, 2001a, b; Carr *et al.*, 2002) and modelling explorations (Chavez *et al.*, 1989; Carr, 2002, 2003; Carr and Kearns, 2003; Echevin *et al.*, 2008). Apart from the modelling studies, descriptions of the phytoplankton community changes have been largely semi-quantitative through the recording of cell abundance changes for different taxonomic groups or the presence of indicator species associated with particular water masses. Off Chile, in the southern Humboldt Current system, ENSO-induced changes in the phytoplankton community and productivity have also been described through shifts in phytoplankton size structure (Iriarte and González, 2004).

The objective of this work is to explore the effect of environmental variability on nearshore phytoplankton biovolume and community dynamics. Long-term detailed sampling of the phytoplankton community in Ancon Bay, located near an important upwelling cell in the central part of the NHCS, provides a unique opportunity to explore these dynamics on a small spatial scale.

METHOD

Sampling

Phytoplankton were collected approximately monthly in Ancon Bay, central Peru (77.65°W–11.2°S) from 1992 to 2004. The sampling station was located on the shelf at a depth of 15 m and ~100 m from the shore (Fig. 1). Samples were taken at three depths (0, 7.5 and 15 m) using a Niskin bottle and phytoplankton were preserved and quantified according to the Utermöhl (Utermöhl, 1958) microscopic method. A subsample of 50 mL was taken and cell counts were conducted to the species

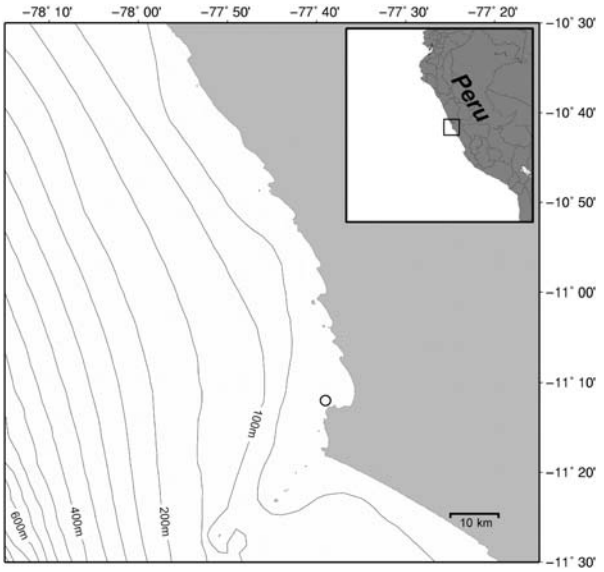

Fig. 1. Map of study area, Ancon Bay, Peru. Circle indicates location of phytoplankton sampling station. Bathymetry data (1 min resolution) is from the GEBCO Digital Atlas of the British Oceanographic Data Centre.

level when possible. In total, 236 taxa were identified. For this study, only the results of the surface samples are presented, yet the analyses of biovolume using averaged sample values from all three depths yielded similar results.

Environmental time series

Environmental time series were first regressed against each other to identify levels of correlation (Pearson). These included five environmental series based on the local water temperature at the time of phytoplankton sampling; absolute temperature at 0 and 15 m ("T0m", "T15m"), temperature anomalies at 0 and 15 m ("T0m_anom", "T15m_anom", °C deviation from monthly means during the sample period 1992–2004) and the Peruvian Oscillation Index (Purca, 2005) ["POI", an index of integrated sea surface temperature (SST) deviations from five coastal sampling stations—Chicama ~4 °S, Paita ~5 °S, Chimbote ~9 °S, Huacho ~11 °S, Callao ~12 °S—along the Peruvian coast. Deviations are based on monthly mean SST values from 1980 to 2006].

Periodicity in environmental time series was explored using a least-squares spectral analysis (LSSA) (or the "Lomb–Scargle method") (Lomb, 1976; Scargle, 1982) within the "nlts" package of the statistical computing software "R" (R Development Core Team, 2008; Bjornstad, 2009). This method determines the least squares fit of sinusoids to a data series, similar to a Fourier analysis; yet, the method is appropriate for unevenly spaced data. Results identify dominant signal peaks in the form of a periodogram.

Biovolume estimation

Abundance data were converted to biovolume using cell dimensions gathered from literature sources or measured by microscopy. Cell dimensions were applied to geometric-shape assignments as described by Hillebrand *et al.* (Hillebrand *et al.*, 1999). Cell biovolume by taxon was calculated using the automated worksheet calculator programmed by Sun and Liu (Sun and Liu, 2003). For further information, see Appendices 1 and 2 in Taylor (Taylor, 2008).

Stepwise multiple regression

A forward stepwise multiple regression procedure was conducted for each taxonomic group using log-transformed biovolume as the dependent variable and environmental time series as independent variables. The initial calculation of correlation coefficients described earlier allowed for the identification of highly interrelated environmental variables, whose significances would be down-weighted if both are included in the resulting regression. The statistical program Statistica 7.0 (StatSoft Inc., 2004) was used, and the procedure settings were left to the default setting, whereby additional variables were added if the regression's cumulative F-value ≥ 1.0.

Community analysis

Community analyses were conducted with the multivariate program, PRIMER 5 (Clarke and Gorley, 2001a). Two matrices of similarity were created, one for the environmental variables and one for biovolume by taxon. As recommended by Clarke and Gorley (Clarke and Gorley, 2001b), environmental data were standardized to account for differing units, but not transformed, and a similarity matrix between samples was created using Euclidean distance. Biovolume data were log-transformed and a similarity matrix of Bray-Curtis similarity was created. Using the PRIMER routine "BIO-ENV", the fixed biotic similarity matrix was compared with environmental similarity matrices considering differing combinations of variables, and correlations between the biotic and environmental similarity matrices were determined (Spearman rank correlation).

Ordinations of samples by multi-dimensional scaling (MDS) were plotted to help visualize sample similarities in terms of community biovolume. The output of MDS coordinates from PRIMER were plotted with the "rgl" package of the statistical computing software "R" (R Development Core Team, 2008; Adler and Murdoch, 2009) in order to colour-code samples along a continuous scale of the environmental values identified by the BIO-ENV routine.

In order to further describe the main community changes, the PRIMER routine "SIMPER" was used to identify taxa that contribute most to community dissimilarity based on *post hoc* environmental factor levels. The contributions of taxa to the dissimilarity between factor levels were then quantified.

RESULTS

Environmental time series

Environmental time series can be seen in Fig. 2, and the matrix of correlation coefficients between time series is shown in Table I. The LSSA revealed that the annual period (i.e. 1.0 year · cycle^{-1}) was the dominant signal of sea surface temperature (T0m), while all other

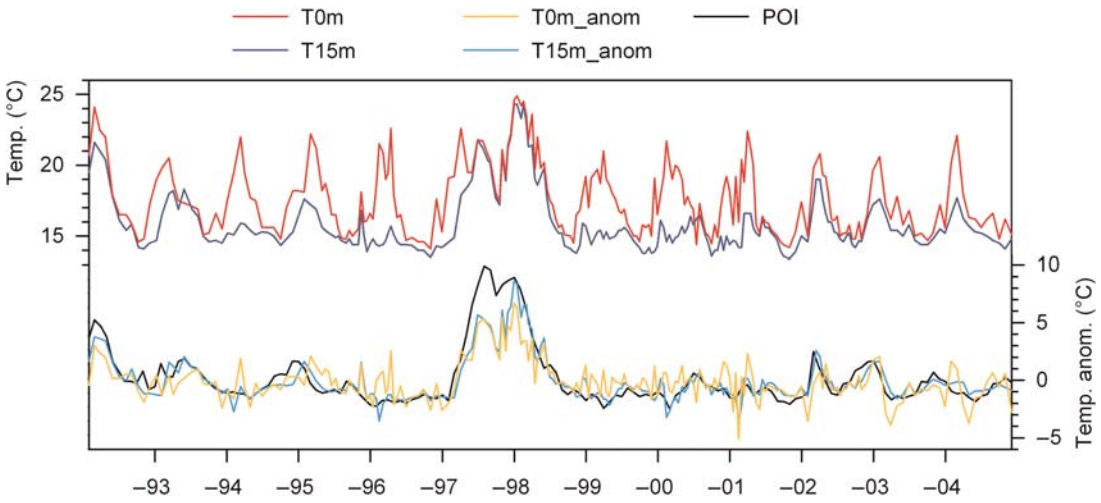

Fig. 2. Time series of absolute temperature and temperature anomalies in Ancon Bay (0 and 15 m), and the Peruvian Oscillation Index (POI) of integrated sea surface temperature anomalies along the Peruvian coast.

Table I: Matrix of correlation coefficients (Pearson) between environmental variables

	T0m	T0m_anom	T15m	T15m_anom	POI
T0m	–				
T0m_anom	0.71	–			
T15m	0.75	0.75	–		
T15m_anom	0.57	0.79	0.94	–	
POI	0.53	0.75	0.85	0.90	–

All correlations are significant at the $P \leq 0.001$ level.

environmental time series had dominant signals at interannual periods (e.g. 5.1 and 8.6 years · cycle^{-1}) (Fig. 3). In particular, the largest peak at 5.1 years · cycle^{-1} for the series T15m, T15m_anom and POI was most obviously related to ENSO periodicities as it approximates the time between the recognized El Niño events in 1991/1992, 1997/1998 and 2002/2003. Both the correlation matrix and the LSSA showed a gradient of environmental variables, from highly local surface water conditions (i.e. T0m) to a regional index of surface water anomalies (i.e. POI). The environmental conditions and dynamics in the deeper waters of Ancon Bay (i.e. T15m and T15m_anom) were also more reflective of the regional, interannual signals.

Biovolume estimation

The contribution of different phytoplankton taxonomic groups to total community biovolume can be seen in Fig. 4. The dynamics through time are highly variable (Fig. 4A), yet it is clear that dinoflagellates and diatoms generally contributed the most to community biovolume. On several intermittent occasions, flagellates were

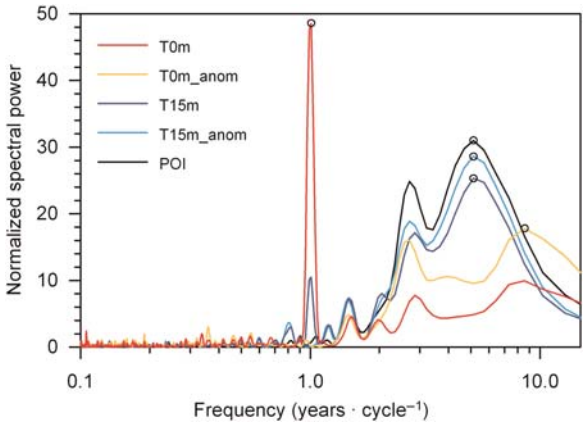

Fig. 3. Periodogram of Ancon Bay environmental time-series by least-squares spectral analysis (LSSA) (the "Lomb–Scargle method"). The dominant peak of each time-series is indicated by a circle symbol. Sea surface temperature (T0m) has a dominant peak at the annual period (1.0 year · cycle^{-1}). All other time series have dominant peaks at interannual periods (5.1 and 8.6 years · cycle^{-1}).

also major contributors to biovolume, whereas silicoflagellates and coccolithophores were not major contributors. Distinct trends can be seen in diatoms and dinoflagellates; specifically, the contribution of diatoms to community biovolume was enhanced during colder T0m (SST) periods and in seasons when strong cold upwelling is typical (i.e. austral winter and spring, months 7–11), while dinoflagellates showed the opposite trend (Fig. 4B and C). Highest total biovolume values were observed during austral summer months (1–3) due to increased dinoflagellate biovolume. Averaging by POI ranges revealed that total biovolume was reduced by ca. 2/3 during periods of strong positive anomalies (i.e. El Niño periods), although the average

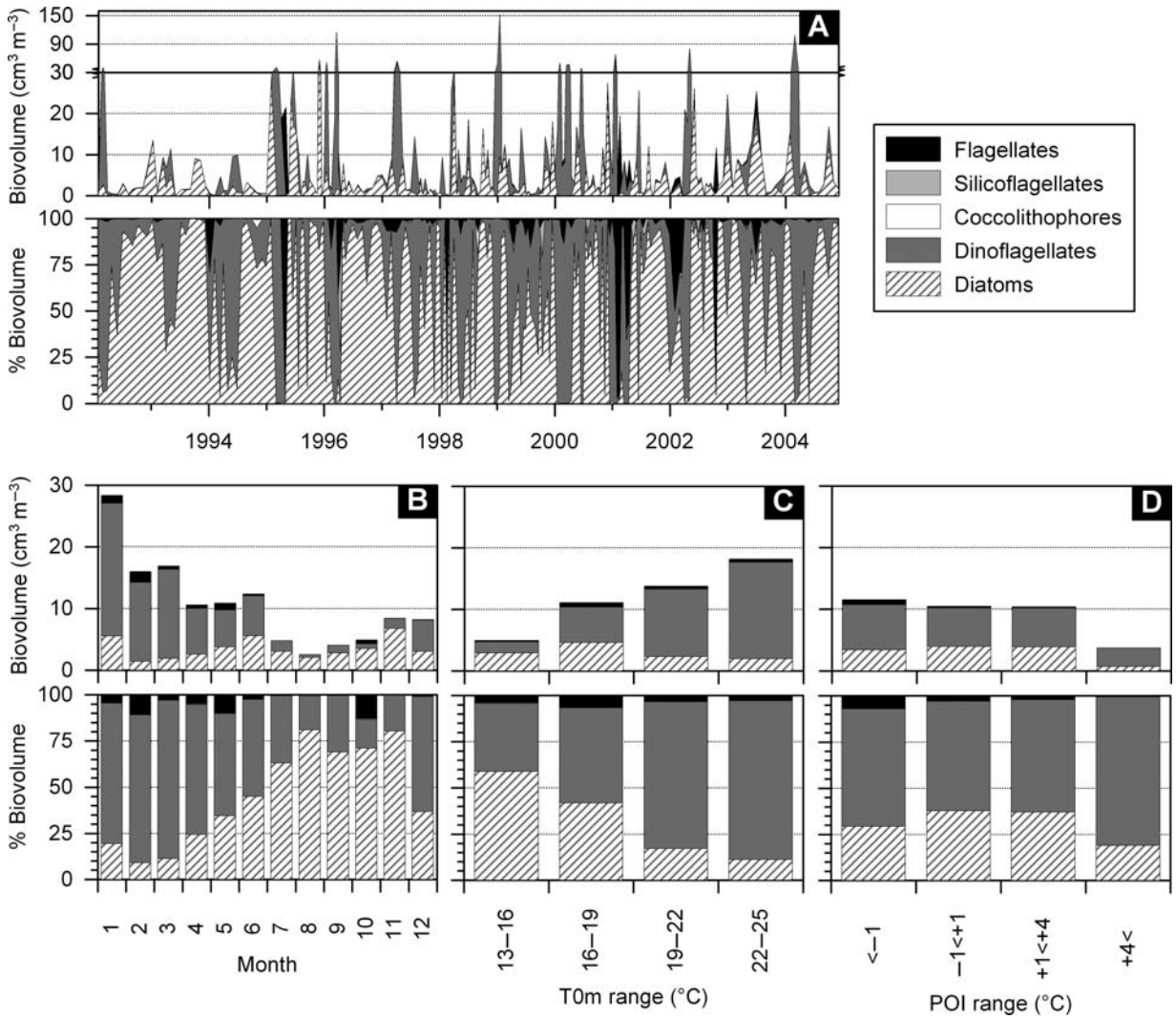

Fig. 4. Calculated biovolume of phytoplankton taxonomic groups. Stacked absolute ($cm^3\ m^{-3}$) and relative (%) biovolumes are displayed for: (**A**) sample date, (**B**) average by month (1=January, 2=February etc.), (**C**) average by T0m (SST) ranges and (**D**) average by POI (peruvian oscillation index) ranges.

relative contributions of phytoplankton taxa were less variable between POI categories (Fig. 4D).

Linear regression

The results of the forward stepwise multiple regression procedure can be seen in Table II. Diatom and dinoflagellate biovolumes were most correlated to the single independent explanatory variable of T0m, which is dominated by annual periodicity. Silicoflagellates correlated best to the single independent explanatory variable of the POI, which is dominated by interannual periodicities. Coccolithophores, flagellates and total phytoplankton biovolumes were correlated to a mix of two independent explanatory variables each. In all cases this included T0m, plus an additional variable of more interannual periodicity; coccolithophores (T0m_anom), flagellates (T15m_anom) and total biovolume (POI). The inclusion of two variables always involved time series of different periodicity and lower correlation, thus providing additional confidence in each signal's significance.

Community analysis

The PRIMER software routine BIO-ENV identified the combination of variables T0m and T15m as those most correlated to the phytoplankton community similarity pattern (Spearman rank correlation; $\rho = 0.134$). The effect of these variables on the MDS plot of community similarity can be visualized by overlaying each variable level separately as a colour gradient (Fig. 5). Due to the high dimensionality of the data and the naturally

Table II: Partial R^2, cumulative R^2, cumulative F and P-level values for each independent abiotic variable (and the sign of its regression coefficient, Pearson) entering the stepwise multiple regression models of the dependent phytoplankton taxonomic groups' biovolume (log-transformed)

Dependent variable	Independent variable	Sign	Partial R^2	Model R^2	F	P-level
Log (biovolume)						
Diatoms ($n = 215$)	T0m[a]	(−)	0.15	0.15	38.70	<0.000000
	T15m_anom	(+)	0.02	0.18	5.72	0.02
Dinoflagellates ($n = 212$)	T0m[a]	(+)	0.10	0.10	24.44	0.000002
	POI	(−)	0.06	0.16	14.35	0.0002
Coccolithophores ($n = 60$)	T0m[a]	(+)	0.05	0.05	2.91	0.09
	T0m_anom[a]	(−)	0.11	0.15	7.09	0.01
Silicoflagellates ($n = 132$)	POI[a]	(−)	0.07	0.07	9.95	0.002
	T15m	(+)	0.05	0.12	6.85	0.01
Flagellates ($n = 181$)	T0m[a]	(+)	0.08	0.08	14.72	0.0002
	T15m_anom[a]	(−)	0.12	0.20	27.52	<0.000000
	T0m_anom	(−)	0.01	0.21	2.22	0.14
	POI	(−)	0.00	0.21	1.06	0.31
Total ($n = 215$)	POI[a]	(−)	0.04	0.04	9.99	0.002
	T0m[a]	(+)	0.06	0.10	13.99	0.0002

[a]Steps where the entry of the independent environmental factor improves the significance of the regression.

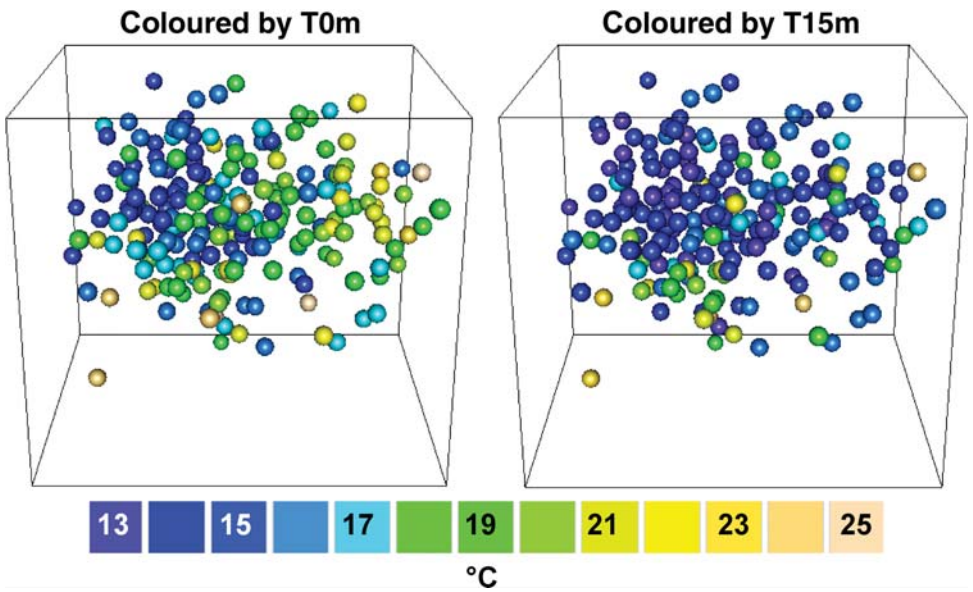

Fig. 5. 3-D MDS plots of Ancon Bay phytoplankton community similarity between samples (spheres, $n = 214$) taken at ca. monthly intervals from 1992 to 2004. Samples with similar community composition (Bray–Curtis similarity) are closer together (stress = 0.20). Both plots represent the same surface phytoplankton community, but are coloured according to temperature recorded at 0 m (left) and 15 m (right) during the time of sampling.

stochastic nature of phytoplankton communities, the "stress" of a 2-D MDS plot (0.26) was deemed too high for a reliable representation of the similarity "distances". A 3-D MDS representation brought the stress level to 0.20, which is at the upper end of the recommended range (Clarke and Warwick, 2001). In general, community samples separated from left to right in accordance with SST, while vertical separation is more related to extreme warming events (e.g. during El Niño events when the temperature at 15 m is also high).

Taxa that contributed most to the dissimilarity in community biovolume between warm and cold SST can be seen in Table III. The top 10 taxa all show higher biovolumes during cold SST conditions. In most cases, average biovolume is several magnitudes higher than during warm conditions. Eight of these top 10 taxa are diatoms, which include: *Actinocyclus octonarius*, *Pleurosigma* sp, *Lithodesmium undulatum*, *Skeletonema costatum*, *Navicula directa* and three *Chaetoceros* species (*C. lorenzianus*, *C. debilis* and *C. curvisetus*). Taxa with higher average

Table III: Taxa contributing most to dissimilarity (upper 50%) between community samples taken at SST 13–16°C vs. 22–25°C

Genus	Species	Group	Group 13–16°C ave. Log(biov.) (μm^3 50 mL^{-1})	Group 22–25°C ave. Log(biov.) (μm^3 50 mL^{-1})	Contrib. %	Cum. %
Actinocyclus	*octonarius*	DIAT.	11.87	3.20	1.95	1.95
Pleurosigma	sp	DIAT.	11.22	4.45	1.74	3.69
Lithodesmium	*undulatum*	DIAT.	9.29	1.83	1.67	5.36
Chaetoceros	*lorenzianus*	DIAT.	9.18	2.03	1.62	6.98
Skeletonema	*costatum*	DIAT.	9.10	2.23	1.62	8.61
Protoperidinium	*mendiolae*	DINO.	9.04	3.47	1.62	10.23
Chaetoceros	*debilis*	DIAT.	7.96	2.91	1.49	11.72
Navicula	*directa*	DIAT.	8.96	6.11	1.40	13.11
Chaetoceros	*curvisetus*	DIAT.	7.86	5.53	1.38	14.50
Gyrodinium	*sp g*	DINO.	6.56	5.96	1.35	15.85
Dyctiocha	*fibula*	SILI.	6.26	7.62	1.33	17.18
Noctiluca	*scintillans*	DINO.	1.98	6.29	1.33	18.51
Coscinodiscus	*perforatus*	DIAT.	6.49	2.58	1.32	19.83
Amphiprora	sp	DIAT.	6.59	6.06	1.30	21.13
Microflagellate	sp	FLAG.	9.47	10.78	1.29	22.42
Glenodinium	sp	DINO.	5.25	5.95	1.29	23.71
Protoperidinium	*longispinum*	DINO.	2.04	6.37	1.28	24.99
Eutreptia	*marina*	FLAG.	3.50	6.75	1.25	26.24
Nitzschia	sp	DIAT.	6.28	3.33	1.25	27.49
Prorocentrum	*gracile*	DINO.	0.64	6.11	1.24	28.73
Thalassionema	*nitzschioides*	DIAT.	7.15	6.84	1.23	29.95
Ceratium	*furca*	DINO.	4.56	7.69	1.20	31.15
Gymnodinium	sp	DINO.	4.15	4.07	1.20	32.35
Cylindrotheca	*closterium*	DIAT.	9.13	7.25	1.19	33.54
Protoperidinium	*minutum*	DINO.	2.46	5.67	1.18	34.72
Gyrodinium	sp	DINO.	6.08	1.61	1.17	35.89
Protoperidinium	*depressum*	DINO.	2.73	5.46	1.15	37.04
Scrippsiella	*trochoidea*	DINO.	2.17	6.20	1.15	38.19
Pseudonitzschia	*delicatissima*	DIAT.	2.62	6.31	1.14	39.33
Chaetoceros	*didymus*	DIAT.	6.15	4.15	1.14	40.47
Cerataulina	*pelagica*	DIAT.	1.99	6.16	1.13	41.60
Thalassiosira	*mendiolana*	DIAT.	6.02	0.65	1.12	42.72
Chaetoceros	*socialis*	DIAT.	5.40	4.89	1.12	43.84
Thalassiosira	*subtilis*	DIAT.	4.81	3.38	1.08	44.92
Leucocryptos	*marina*	FLAG.	1.26	5.42	1.04	45.95
Gyrosigma	sp	DIAT.	4.85	3.68	0.99	46.95
Prorocentrum	*micans*	DINO.	0.73	5.2	0.99	47.94
Thalassiosira	*anguste-lineata*	DIAT.	4.84	1.64	0.98	48.92
Guinardia	*delicatula*	DIAT.	3.88	4.34	0.98	49.90
Eucampia	*zoodiacus*	DIAT.	4.44	2.69	0.97	50.87

biovolume during warm conditions were predominantly dinoflagellates, flagellates and silicoflagellates. These included the dinoflagellates: *Ceratium furca, Noctiluca scintillans, Prorocentrum gracile, Prorocentrum micans, Scrippsiella trochoidea* and three *Protoperidinium* species (*P. longispinum, P. minutum and P. depressum*). Top contributing flagellates (Microflagellate sp, *Eutreptia marina* and *Leucocryptos marina*) and silicoflagellates (*Dyctiocha fibula*) all showed higher biovolumes during warm SST conditions.

DISCUSSION

General trends in phytoplankton biovolume

Despite the highly variable nature of the phytoplankton community in Ancon Bay that we observed (Fig. 4A), the trends in total biovolume and contribution by taxa are consistent with previous descriptions for the Humboldt Current system. The yearly cycle in total biovolume, showing highest values during summer–autumn months and lowest values during winter months, has also been estimated through remote sensing (SeaWiFS) of chlorophyll off Peru (Thomas *et al.*, 2001a, b; Echevin *et al.*, 2008). Lower chlorophyll *a* levels during winter months in the larger Peruvian upwelling system are also observable *in situ* (Montecino *et al.*, 2006; Pennington *et al.*, 2006; Echevin *et al.*, 2008). Generally, increased chlorophyll levels in the Humboldt Current system begin earlier in spring with a slightly later summer–autumn peak than the observed biovolume peak in Ancon Bay. Modelling explorations of the larger Peruvian system attribute these seasonal peaks in chlorophyll to the dynamics of nutrient

availability (via upwelling) in combination with destratification–restratification dynamics resulting from changes in the depth of the mixed layer. Specifically, increased surface winds during winter deepen the mixed layer and reduce the surface chlorophyll accumulation due to a dilution effect and light limitation (Echevin *et al.*, 2008). In north-central Chile, highest chlorophyll levels are also observed during more neutral rather than cold upwelling periods, suggesting that transitional periods with less turbulent mixing can result in higher phytoplankton biomass (Montecino *et al.*, 2006). For the shallow nearshore habitat of Ancon Bay, some temperature stratification is also visible during summer months, which may indicate a decrease in the mixed layer depth and help explain the increase in surface biovolume. Nevertheless, the accompanying shift toward a higher proportion of dinoflagellates would indicate that additional factors are involved.

Diatoms have previously been described as the most abundant primary producer during all seasons for the area within 5 miles of the Peruvian coast (Rojas de Mendiola, 1981); yet, from a biovolume perspective, diatoms appear to dominate the nearshore community only under strong cold upwelling conditions. Under reduced upwelling conditions, as are commonly observed during austral summer and autumn, dinoflagellates contribute more on average to total biovolume levels. Part of this inconsistency may be due to the fact that previous descriptions were based on cell abundances rather than biovolume. Diatom species in early phytoplankton successional stages may be smaller, fast-growing species and thus their high numbers may not directly translate into biovolume.

Also consistent with previous remote sensing estimates is an overall reduction in phytoplankton during strong El Niño events. Total phytoplankton biovolume in Ancon Bay during periods of high temperature anomalies was about one-third the level of other periods. While there was a reduction in the proportion of diatoms during these periods, the effect is not as strong as for increased SST.

Local vs. regional influences on the phytoplankton taxonomic groups

The results of the spectral analysis (Fig. 3) indicate that the environmental variables may be divided into two main categories: (i) large scale, more regionally affected signals with highest variability at interannual ENSO scales (e.g. temperature anomalies and temperature at 15 m depth) and (ii) local signals reflecting intra-annual upwelling variability (e.g. SST). These two categories will be considered in the following sections describing the influence of the environment on phytoplankton community dynamics.

The inclusion of more regional factors significantly improves the correlation of total phytoplankton biovolume and coccolithophore, silicoflagellate and flagellate groups. In all cases, the correlation coefficient is negative (Table II); i.e. positive temperature anomalies result in lower biovolume. Similarly, the BIO-ENV routine also identifies that temperature at 15 m is correlated to the community pattern, contributing to the vertical separation in the MDS plot (Fig. 5). Along the coast of Peru, an overall reduction in nutrient availability to the euphotic zone occurs during strong El Niño events (e.g. 1997/1998); specifically, the arrival of a Kelvin wave to the Peruvian coast elevates sea level, which results in a depression of the thermocline (Chavez *et al.*, 1989; Philander, 1990). While upwelling may continue, the lowered thermocline prevents the deeper, nutrient-rich water from reaching the euphotic zone (Barber and Smith, 1981; Chavez *et al.*, 1989). Thus, ENSO-related interannual variability most likely affects large-scale nutrient availability, although local upwelling is ultimately needed to bring these nutrients to the euphotic zone.

At the local scale, changes in SST significantly contribute to the correlation of all groups except silicoflagellates (Table II). The high intra-annual variability of SST is more reflective of local wind-forced upwelling, affecting the vertical and cross-shelf transport of water and nutrients. Diatoms show the strongest (negative) correlation, which is consistent with previous observations of high diatom density in cold water upwelling cells (Strickland *et al.*, 1969). As Ancon Bay is located within one of three main, semi-permanent upwelling cells along the coast of Peru: Tumbes-Paita (5°), Huacho-Callao (11°–12°) and Pisco (15°) (Maeda and Kishimoto, 1970; Zuta and Guillen, 1970), increased diatom biovolume is likely to result from local upwelling processes rather than import from other areas. High diatom concentrations in upwelling zones have often been attributed to physiological or competitive adaptations to the nutrient-rich conditions (e.g. higher production rates); however, there is increasing evidence that physical processes may play a more significant role in the observed distribution patterns. For example, vertical velocity has been shown to be an important factor in determining phytoplankton size spectra (Rodriguez *et al.*, 2001) with a shift towards larger cell sizes under strong vertical velocities. Diatoms are large in size or have the ability to form chains or other cell aggregates, which particularly facilitate vertical transport during upwelling. Furthermore, the ability to form resting spores during oligotrophic conditions, which sink and

are subsequently returned to the surface via upwelling (Pitcher *et al.*, 1992), allows them to maintain their spatio-temporal position in the upwelling zone rather than continuing to be transported offshore. Alternatively, dinoflagellates, coccolithophores and flagellates are normally found in higher abundances offshore in association with warm subtrophical waters (Rojas de Mendiola, 1981; Avaria and Muñoz, 1987; Barber and Kogelschatz, 1990) and represent later successional stages of the phytoplankton community (Cushing, 1989). Their presence in the near coastal zone has been observed to coincide with periods of reduced upwelling (Rojas de Mendiola, 1981; Ochoa *et al.*, 1985; Avaria and Muñoz, 1987). Due to their smaller size and high surface to volume ratios, they are likely to have some advantage in nutrient uptake under oligotrophic conditions; nevertheless, their increased presence inshore is probably also facilitated by physical processes. Off Peru, underlying geostrophic forces are directed onshore (Parrish *et al.*, 1983; Colas *et al.*, 2008) and during periods of decreased upwelling and Ekman transport, offshore water from beyond the shelf may intrude into the nearshore environment and brings with it the associated phytoplankton community.

The consistency across methodologies in identifying correlations between environmental signals and biovolume and community changes allows for a greater degree of confidence in the results. Furthermore, to the authors' knowledge, the use of a community matrix of 224 samples by 236 taxa is one of the largest employed in a community analysis; yet, the creation of a meaningful 3-D MDS plot, with consistent results between the BIO-ENV routine and the stepwise multiple regression, gives weight to the methods' use in a wide variety of community sampling regimes.

Characterizing features of community dynamics

The community changes observed in Ancon Bay are in agreement with previous findings in the Humboldt Current system in that diatoms dominate the system during strong upwelling periods (typically in winter and spring), whereas dinoflagellates and other smaller sized flagellates are found during weakened upwelling periods (typically summer and autumn) and El Niño periods when nutrient availability is limited (Iriarte *et al.*, 1995, 2000; González *et al.*, 2004; Iriarte and González, 2004; Montecino *et al.*, 2006). SST was also found to be an important predictor for biovolume in other phytoplankton groups and for the community as a whole (Table II). The following sections describe the taxa that contribute most to the differences in the community between cold and warm SST conditions (Table III).

Characteristic taxa of cold upwelling periods include several of the diatom genus *Chaetoceros*. This genus is known to respond quickly to mixing events (Eppley *et al.*, 1969; Margalef, 1978), is typical of the coastal phytoplankton assemblage in both Peru and Chile (Romero and Hebbeln, 2003; Abrantes *et al.*, 2007) and is especially abundant during spring upwelling events in Peru (Rojas de Mendiola, 1981). *Actinocyclus octonarius* and *Skeletonema costatum* are also typical diatom species of the coastal phytoplankton assemblage in Chile and Peru (Abrantes *et al.*, 2007). *Skeletonema costatum* is especially adapted to react quickly to freshly upwelled waters through high rates of production and nutrient uptake (Conway, 1977; Conway and Harrison, 1977; Serra *et al.*, 1978). In Chile, valves *of S. costatum* in sediments are only narrowly distributed under specific upwelling centres (34–37°S) (Romero and Hebbeln, 2003), thus making it a good indicator species for recently upwelled water.

Characteristic dinoflagellate species of warm conditions included four mixotrophic red tide-causing species (*Ceratium furca, Prorocentrum gracile, P. micans* and *Scrippsiella trochoidea*; Note: *S. trochidae* has not been observed to cause red tides in Peru) and several heterotrophic species (*Noctiluca scintillans, Protoperidinium longispinum, P. minutum* and *P. depressum*). Generally, increases in later successional stages (dinoflagellates, flagellates and silicoflagellates) during warm conditions are likely to be either a result of decreased offshore transport or an intrusion of offshore waters to the nearshore area of Ancon Bay. An upwelling relaxation and/or reversal would prevent the new production of species more adapted to the high nutrient conditions (i.e. small chain-forming diatoms) and allow for the development of later phytoplankton successional stages with more mixed or heterotrophic diets (Cushing, 1989). In addition, we observed that some species are usually only associated with the initial onset of a warming event (e.g. *C. furca* and *P. depressum*), indicating succession within the dinoflagellate group itself.

The schema in Fig. 6 illustrates how the observed nearshore community and biovolume dynamics might result from environmental forcing. Using the same main axes of separation in the MDS plot of community similarity, phytoplankton structures attributable to intra-annual variability are from left to right, while structures attributable to interannual ENSO variability are from top to bottom. Intra-annual variability is mainly due to changes in local wind-forced upwelling, which also affects the degree of offshore transport and the depth of the mixing layer. Interannual variability is related to the phase of

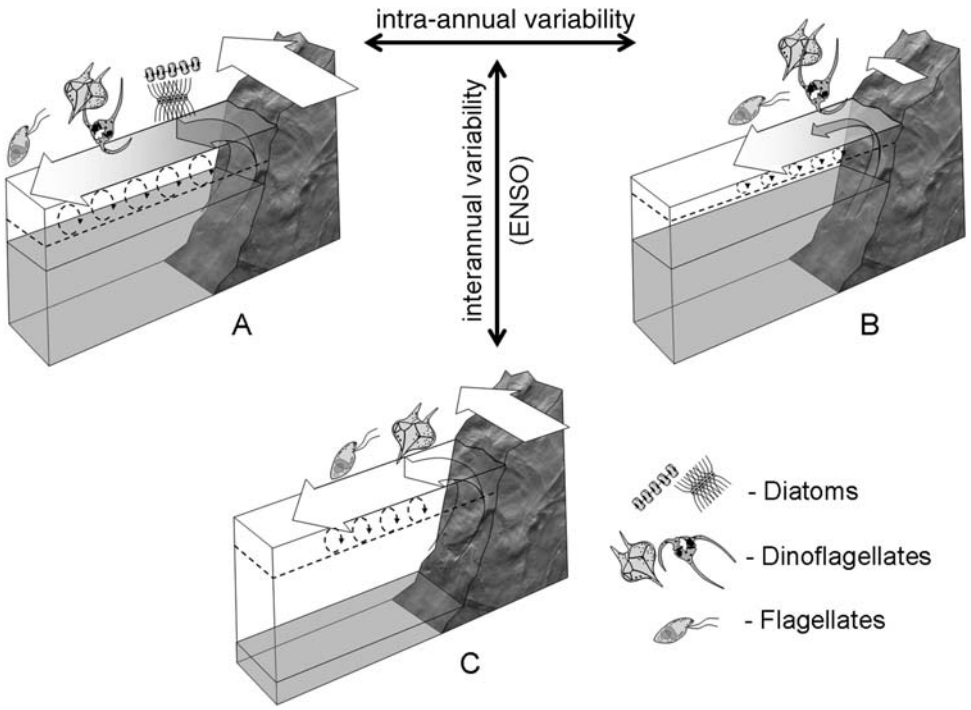

Fig. 6. Schema of intra- and interannual production in the northern Humboldt Current system. The thermocline is represented by the separation between the clear and shaded layers; the shaded layer being cold, nutrient-rich water below the thermocline. The strength of the alongshore wind (solid white arrow) affects the depth of the mixed layer (dashed line) and the degree of perpendicular offshore water movement and subsequent upwelling. (**A**) Strong upwelling, ENSO neutral/La Niña—typical "cold" period characterized by high nutrient availability, stronger mixing and offshore transport, dominance of small diatoms in the nearshore area and later successional stages (e.g. dinoflagellates and other flagellates) found further offshore as nutrients are depleted. (**B**) Weak upwelling, ENSO neutral/La Niña—a "warm" period characterized by lower nutrient availability, reduced local upwelling/relaxation, weaker mixing and offshore transport, dominance of dinoflagellates in the nearshore area. (**C**) El Niño—a "warm" period characterized by a prolonged lowering of the thermocline that prevents the upwelling of cold, nutrient-rich waters. Overall biovolume of phytoplankton is dramatically reduced and more mixotrophic and heterotrophic species of phytoplankton are dominant.

ENSO, which results in regional changes in the depth of the thermo-nutricline. The schema combines some elements of illustrations by Cushing (Cushing, 1989) concerning the phytoplankton succession in upwelling zones with that of R.T. Barber in Canby (Canby, 1984) regarding the effect of El Niño on the depth of the thermo-nutricline and subsequent primary production. In addition to these processes, we have also included the effect of local wind strength on the depth of the mixed layer, which appears to have a significant effect on the concentration (or dilution) of plankton in the upper layers of the water column. As mentioned earlier, our findings concur with other studies that the highest levels of surface phytoplankton biomass are likely to be a result of a reduced mixed layer depth.

Significance for the dynamics of the Humboldt Current ecosystem

Our results indicate a decrease in the larger size fraction of phytoplankton (i.e. diatoms) during periods of decreased upwelling (as reflected by warmer SST). Previous studies have associated these phytoplankton changes with upwelling and ENSO variability (Iriarte and González, 2004); yet, our findings suggest that local upwelling variability is the more important of the two factors. A shift towards smaller-celled phytoplankton is thought to result in changes for the entire food web, with energy passing through alternative pathways before reaching a particle size suitable for grazing by small pelagic fishes (Sommer *et al.*, 2002; González *et al.*, 2004; van der Lingen *et al.*, 2006). From this trophic perspective, one would expect that the most direct transfer of energy to grazing fish occurs during the winter to spring months when diatom biovolume is highest. In fact, increased zooplankton concentrations (Carrasco and Lozano, 1989; Ayón *et al.*, 2004), increased anchovy fat content (Tsukayama, 1989) and the major spawning peak (July to September) all occur during this period (Pauly and Soriano, 1987; Peña *et al.*, 1989). Small pelagic fish grazing efficiency is hypothesized to also be enhanced during periods of upwelling due to a

shallower thermocline, which would concentrate plankton within a narrower active feeding depth (Chavez and Messié, 2009).

Interestingly, despite the apparent trophic advantages associated with strong upwelling periods, the anchovy's main yearly recruitment is predicted to result from the lesser of the two spawning peaks, which occurs in February and March (Mendelssohn and Mendo, 1987; Pauly, 1987). Based on the data for Ancon Bay, this period corresponds to warmer periods when the phytoplankton community is dominated by dinoflagellates, indicating offshore intrusions or reduced offshore transport. It is possible that this period would also be favourable for the retention of anchovy eggs in the coastal zone, which would explain the disproportionate recruitment success following the summer spawning peak.

Thus, seasonal upwelling variability is shown to affect phytoplankton community dynamics on small spatial scales and may possibly aid in the recruitment dynamics of some broadcast spawning organisms through increased retention of eggs and larvae. Due to the higher frequency of seasonal variability, bottom-up trophic effects are probably of lesser importance than the large scale, lower frequencies associated with ENSO. Nevertheless, similarities exist between the phytoplankton community during summer and El Niño events, due in part to a physical intrusion of offshore waters. In addition to changes in the phytoplankton community, associated flora and fauna of the warmer subtropical waters can also occur closer to shore. One example is the comparable shift towards a more coastal spatial distribution of the typically offshore-associated mackerels during summer and El Niño events (Muck and Sanchez, 1987). While these onshore migrations have been shown to affect the dynamics of the more coastal resources on interannual scales (Taylor *et al.*, 2008), their analogous response on seasonal scales suggests that important top–down interactions may also occur at higher frequencies.

ACKNOWLEDGEMENTS

The authors wish to thank the following people: Dr Werner Wosniok for helpful advice on conducting the regression analyses; Dr Bettina Schmitt for helpful suggestions on improving the earlier manuscript; two anonymous reviewers whose critique and suggestions were very helpful in improving the manuscript. The authors wish to acknowledge use of the Maptool program for the creation of the map figure in this paper. Maptool is a product of SEATURTLE.ORG. (Information is available at www.seaturtle.org).

FUNDING

This study was partly financed and conducted in the frame the EU-project CENSOR (Climate variability and EI Niño Southern Oscillation: Impacts for natural resources and management, contract No. 511071).

REFERENCES

Abrantes, F., Lopesa, C., Mix, A. *et al.* (2007) Diatoms in Southeast Pacific surface sediments reflect environmental properties. *Quat. Sci. Rev.*, **26**, 155–169.

Adler, D. and Murdoch, D. (2009) *rgl: 3D Visualization Device System (OpenGL)*. R package version 0.84. http://rgl.neoscientists.org.

Avaria, S. and Muñoz, P. (1987) Effects of the 1982–1983 El Niño on the marine phytoplankton off northern Chile. *J. Geophys. Res.*, **92**, 14369–14382.

Ayón, P., Purca, S. and Guevara-Carrasco, R. (2004) Zooplankton volume trends off Peru between 1964 and 2001. *ICES J. Mar. Sci.*, **61**, 478–484.

Bakun, A. (1996) *Patterns in the Ocean. Ocean Processes and Marine Population Dynamics*. University of California Sea Grant, California, USA, in cooperation with Centro de Investigaciones Biologicas de Noroeste, La Paz, Baja California Sur, Mexico.

Bakun, A. and Weeks, S. J. (2008) The Marine Ecosystem off Peru: what are the secrets of its fishery productivity and what might its future hold? *Prog. Oceanogr.*, **79**, 290–299.

Barber, R. and Kogelschatz, J. (1990) Nutrients and Productivity during the 1982/83 El Niño. In Glyn, P. (ed.), *Global Ecological Consequences of the 1982–1983 El Niño-Southern Oscillation.* Vol. 52. Elsevier, Amsterdam, pp. 21–53.

Barber, R. T. and Smith, R. L. (1981) Coastal upwelling ecosystems. In Longhurst, A. R. (ed.), *Analysis of Marine Ecosystems*. Academic Press, New York, pp. 31–68.

Bjornstad, O. N. (2009) *nlts: (Non)linear Time Series Analysis*. R package version 0.1-5.

Canby, T. Y. (1984) *El Niño: Global Weather Disaster.* National Geographic Magazine, Vol. 165, 144–183.

Carr, M. E. (2002) Estimation of potential productivity in eastern boundary currents using remote sensing. *Deep-Sea Res. (Part II, Top. Stud. Oceanogr.)*, **49**, 59–80.

Carr, M. E. (2003) Simulation of carbon pathways in the planktonic ecosystem off Peru during the 1997–1998 El Niño and La Niña. *J. Geophys. Res. (C Oceans)*, **108**, 3380.

Carr, M. E. and Kearns, E. J. (2003) Production regimes in four Eastern Boundary Current systems. *Deep-Sea Res. II Top. Stud. Oceanogr.*, **50**, 3199–3221.

Carr, M. E., Strub, P. T., Thomas, A. C. *et al.* (2002) Evolution of 1996–1999 La Niña and El Niño conditions off the western coast of South America: a remote sensing perspective. *J. Geophys. Res. (C Oceans)*, **107**, 1–16.

Carrasco, S. and Lozano, O. (1989) Seasonal and long-term variations of zooplankton volumes in the Peruvian Sea, 1964–1987. In Pauly, D., Muck, P., Mendo, J., Tsukayama, I. *et al.* (eds), *The Peruvian Upwelling Ecosystem: Dynamics and Interactions*. Vol. 18. *ICLARM Conference Proceedings*, Manila, Philippines, pp. 82–85.

Chavez, F. and Messié, M. (2009) A comparison of Eastern Boundary Upwelling Ecosystems. *Prog. Oceanogr.*, **83**, 80–96.

Chavez, F. P., Barber, R. T. and Sanderson, M. P. (1989) The potential primary production of the Peruvian upwelling ecosystem, 1953–1984. In Pauly, D., Muck, P., Mendo, J., Tsukayama, I. *et al.* (eds), *The Peruvian Upwelling Ecosystem: Dynamics and Interactions*. Vol. 18. *ICLARM Conference Proceedings*. Manila, Philippines, pp. 50–63.

Clarke, K. R. and Gorley, R. N. (2001a) *PRIMER 5*. version 5.2.2. PRIMER-E Ltd, Plymouth, UK. http://www.primer-e.com/.

Clarke, K. R. and Gorley, R. N. (2001b) *PRIMER v5: User Manual/Tutorial*. PRIMER-E, Plymouth, UK.

Clarke, K. R. and Warwick, R. M. (2001) *Changes in Marine Communities: An Approach to Statistical Analysis and Interpretation*, 2nd edition. PRIMER-E Ltd, Plymouth, UK.

Colas, F., Capet, X., McWilliams, J. C. *et al.* (2008) 1997–1998 El Niño off Peru: a numerical study. *Prog. Oceanogr.*, **79**, 138–155.

Conway, H. L. (1977) Interactions of inorganic nitrogen in the uptake and assimilation by marine phytoplankton. *Mar. Biol.*, **39**, 221–232.

Conway, H. L. and Harrison, P. J. (1977) Marine diatoms grown in chemostats under silicate or ammonium limitation. IV. Transient response of Chaetoceros debilis, Skeletonema constatum, and Thalassiosira gravida to a single addition of the limiting nutrient. *Mar. Biol.*, **43**, 33–43.

Cury, P., Roy, C. and Faure, V. (1998) Environmental constraints and pelagic fisheries in upwelling areas: the Peruvian puzzle. *S. Afr. J. Mar. Sci./Suid-Afrikaanse Tydskrif vir Seewetenskap*, **19**, 159–167.

Cushing, D. H. (1989) A difference in structure between ecosystems in strongly stratified waters and in those that are only weakly stratified. *J. Plankton Res.*, **11**, 1–13.

Echevin, V., Aumont, O., Ledesma, J. *et al.* (2008) The seasonal cycle of surface chlorophyll in the Peruvian upwelling system: A modelling study. *Prog. Oceanogr.*, **79**, 167–176.

Eppley, R., Rogers, J. and McCarthy, J. (1969) Half saturation constant for uptake of nitrate and aluminium by marine phytoplankton. *Limnol. Oceanogr.*, **14**, 912–920.

Fréon, P., Barange, M. and Arístegui, J. (2009) Eastern boundary upwelling ecosystems: integrative and comparative approaches. *Prog Oceanogr.*, **83**, 1–14.

Goldberg, S. B. and O'Brien, J. J. (1981) Time and space variability of tropical Pacific wind stress. *Mar. Weather Rev.*, **109**, 1190–1207.

González, H. E., Giesecke, R., Vargas, C. A. *et al.* (2004) Carbon cycling through the pelagic foodweb in the northern Humboldt Current off Chile (23 degrees S). *ICES J. Mar. Sci.*, **61**, 572–584.

Hillebrand, H., Duerselen, C. D., Kirschtel, D. *et al.* (1999) Biovolume calculation for pelagic and benthic microalgae. *J. Phycol.*, **35**, 403–424.

Iriarte, J. L. and González, H. E. (2004) Phytoplankton size structure during and after the 1997/98 El Nino in a coastal upwelling area of the northern Humboldt Current System. *Mar. Ecol. Prog Ser.*, **269**, 83–90.

Iriarte, J. L., Uribe, J. C. and Valladares, C. (1995) Biomass of size-fractionated phytoplankton during the spring-summer season in southern Chile. *Bot. Mar.*, **36**, 443–450.

Iriarte, J. L., Pizarro, G., Troncoso, V. A. *et al.* (2000) Primary production and biomass of size-fractionated phytoplankton off Antofagasta, Chile (23–24°S) during pre-El Niño and El Niño 1997. *J. Mar. Syst.*, **26**, 37–51.

Lomb, N. R. (1976) Least-squares frequency-analysis of unequally spaced data. *Astrophys. Space Sci.*, **39**, 447–462.

Maeda, S. and Kishimoto, R. (1970) Upwelling off the Coast of Peru. *J. Oceanogr. Soc. Jpn*, **26**, 300–309.

Margalef, R. (1978) Life-forms of phytoplankton as survival alternatives in an unstable environment. *Oceanol. Acta*, **1**, 493–509.

Mendelssohn, R. and Mendo, J. (1987) Exploratory analysis of anchoveta recruitment off Peru and related environmental series. In Pauly, D. and Tsukayama, I. (eds), *The Peruvian Anchoveta and Its Upwelling Ecosystem: Three Decades of Change*. ICLARM, Manila, Philippines, pp. 294–306.

Montecino, V. and Lange, C. B. (2009) The Humboldt Current System: ecosystem components and processes, fisheries, and sediment studies. *Prog. Oceanogr.*, **83**, 65–79.

Montecino, V., Paredes, M. A., Paolini, P. *et al.* (2006) Revisiting chlorophyll data along the coast in north-central Chile, considering multiscale environmental variability. *Rev. Chil. Hist. Nat.*, **79**, 213–223.

Montecinos, A., Purca, S. and Pizarro, O. (2003) Interannual-to-interdecadal sea surface temperature variability along the western coast of South America. *Geophys. Res. Lett.*, **30**, 1–4.

Muck, P. and Sanchez, G. (1987) The importance of mackerel and horse mackerel predation for the Peruvian anchoveta stock (a population and feeding model). In Pauly, D. and Tsukayama, I. (eds), *The Peruvian Anchoveta and Its Upwelling Ecosystem: Three Decades of Change*. Vol. 391. ICLARM, Manila, Philippines, pp. 276–293.

Myers, G. (1979) Annual variation in the slope of the 14°C isotherm along the equator in the Pacific Ocean. *J. Phys. Oceanogr.*, **9**, 885–891.

Ochoa, N., Rojas de Mendiola, B. and Gómez, O. (1985) Identificación del fenómeno El Niño a través de los organismos fitoplanctónicos. *Book Identificación del fenómeno El Niño a través de los organismos fitoplanctónicos*. Instituto del Mar del Perú (IMARPE), pp. 22–32.

Parrish, R. H., Bakun, A., Husby, D. M. *et al.* (1983) Comparative climatology of selected environmental processes in relation to eastern boundary current pelagic fish reproduction. In Sharp, G. D. and Csirke, J. (eds), *Proceedings of the Expert Consultation to Examine Changes in Abundance and Species Composition of Neritic Fish Resources*. Vol. 291, FAO Fisheries Report. San Jose, Costa Rica, pp. 731–777.

Pauly, D. (1987) Managing the Peruvian upwelling ecosystem: a synthesis. In Pauly, D. and Tsukayama, I. (eds), *The Peruvian Anchoveta and Its Upwelling Ecosystem: Three Decades of Change*. Vol. 391. ICLARM, Manila, Philippines, pp. 325–342.

Pauly, D. and Soriano, M. (1987) Monthly spawning stock and egg production of Peruvian anchoveta (Engraulis ringens) 1953 to 1982. In Pauly, D. and Tsukayama, I. (eds), *The Peruvian Anchoveta and Its Upwelling Ecosystem: Three Decades of Change*. Vol. 391. ICLARM, Manila, Philippines, pp. 167–178.

Peña, N., Mendo, J. and Pellón, J. (1989) Sexual maturity of Peruvian anchoveta (*Engraulis ringens*), 1961–1987. In Pauly, D., Muck, P., Mendo, J., Tsukayama, I. *et al.* (eds), *The Peruvian Upwelling Ecosystem: Dynamics and Interactions*. *Vol. 18. ICLARM Conferences Proceedings*. Manila, Philippines, pp. 132–142.

Pennington, J. T., Mahoney, K. L., Kuwahara, V. S. *et al.* (2006) Primary production in the eastern tropical Pacific: a review. *Prog Oceanogr.*, **69**, 285–317.

Philander, S. G. (1990) *El Niño, La Niña, and the Southern Oscillation*. Academic Press, San Diego.

Pitcher, G. C., Brown, P. C. and Mitchell-Innes, B. A. (1992) Spatio-temporal variability of phytoplankton in the southern Benguela Upwelling system. *S. Afr. J. Mar. Sci.*, **12**, 439–456.

Purca, S. (2005) Variabilidad temporal de baja frecuencia en el Ecosistema de la Corriente de Humboldt frente a Perú. PhD Thesis. Universidad de Concepción.

R Development Core Team. (2008) *R: A Language and Environment for Statistical Computing*. R Foundation for Statistical Computing, Vienna, Austria, ISBN 3-900051-07-0, http://www.R-project.org.

Rodriguez, J., Tintore, J., Allen, J. T. *et al.* (2001) Mesoscale vertical motion and the size structure of phytoplankton in the ocean. *Nature*, **410**, 360–363.

Rojas de Mendiola, S. (1981) Seasonal phytoplankton distribution along the Peruvian coast. In Richards, F. A. (ed.), *Coastal Upwelling*. Vol. 20. American Geophysical Union, Washington, D.C, pp. 348–356.

Romero, O. and Hebbeln, D. (2003) Biogenic silica and diatom thanatocoenosis in surface sediments below the Preu-Chile Current: controlling mechanisms and relationship with productivity in surface waters. *Mar. Micropaleontol.*, **48**, 71–90.

Scargle, J. D. (1982) Studies in astronomical time series analysis. II—Statistical aspects of spectral analysis of unevenly spaced data. *Astrophys. J.*, **263**, 835–853.

Serra, J. L., Llama, M. J. and Cadenas, E. (1978) Nitrate utilization by the diatom skeletonema costatum: I. Kinetics of nitrate uptake. *Plant Physiol.*, **62**, 987–990.

Sommer, U., Stibor, H., Katechakis, A. *et al.* (2002) Pelagic food web configurations at different levels of nutrient richness and their implications for the ratio fish production:primary production. *Hydrobiologia*, **484**, 11–20.

StatSoft Inc (2004) *STATISTICA (Data Analysis Software System), version 7*. www.statsoft.com.

Strickland, J. D. H., Eppley, R. W. and Rojas be Mendiola, B. (1969) Phytoplankton populations, nutrients and photosynthesis in Peruvian coastal waters. *Bol. Inst. Mar. Peru*, **2**, 4–45.

Sun, J. and Liu, D. (2003) Geometric models for calculating cell biovolume and surface area for phytoplankton. *J. Plankton Res.*, **25**, 1331–1346.

Tam, J., Taylor, M. H., Blaskovic, V. *et al.* (2008) Trophic modeling of the northern Humboldt Current Ecosystem, Part I: comparing trophic linkages under La Niña and El Niño conditions. *Prog. Oceanogr.*, **79**, 352–365.

Taylor, M. H. (2008) The Northern Humboldt Current Ecosystem and its resource dynamics: Insights from a trophic modeling and time series analysis. PhD Thesis. Bremen University.

Taylor, M. H., Tam, J., Blaskovic, V. *et al.* (2008) Trophic modeling of the Northern Humboldt Current Ecosystem, Part II: elucidating ecosystem dynamics from 1995 to 2004 with a focus on the impact of ENSO. *Prog. Oceanogr.*, **79**, 366–378.

Thomas, A. C., Blanco, J. L., Carr, M. E. *et al.* (2001a) Satellite-measured chlorophyll and temperature variability off northern Chile during the 1996–1998 La Nina and El Nino. *J. Geophys. Res. (C Oceans)*, **106**, 899–915.

Thomas, A. C., Carr, M.-E. and Strub, P. T. (2001b) Chlorophyll variability in eastern boundary currents. *Geophys. Res. Lett.*, **28**, 3421–3424.

Tsukayama, I. (1989) Dynamics of the Fat Content of Peruvian Anchoveta (Engraulis ringens). In Pauly, D., Muck, P., Mendo, J., Tsukayama, I. *et al.* (eds), *The Peruvian Upwelling Ecosystem: Dynamics and Interactions*. Vol. 18. *ICLARM Conference Proceedings*. Manila, Philippines, 125–131.

Utermöhl, H. (1958) Zur Vervollkommnung der quantitativen Phytoplankton-Methodik. *Int. Ver. Theor. Angewandte Limnol. Mitt.*, **9**, 1–38.

van der Lingen, C. D., Hutchings, L. and Field, J. G. (2006) Comparative trophodynamics of anchovy Engraulis encrasicolus and sardine Sardinops sagax in the southern Benguela: are species alternations between small pelagic fish trophodynamically mediated. *Afr. J. Mar. Sci.*, **28**, 465–477.

Zuta, S. and Guillen, O. (1970) Oceanografía de las aguas costeras del Peru. *Bol. Inst. Mar. Perú*, **2**, 157–324.